Theoretical resistance in cylindrical electrodes with conical tip

Chang-Ho Hong[1a], Jin-Seop Kim[1b] and Song-Hun Chong[*2]

*[1]Disposal Performance Demonstration Research Division, Korea Atomic Energy Research Institute,
111, Daedeok-daero 989, Yuseong-gu, Daejeon, 34057, Republic of Korea*
[2]Department of Civil Engineering, Sunchon National University, 255 Jungang-ro, Sunchon, 57922, Republic of Korea

Abstract. The electrical resistivity method is a well-known geophysical method for observing underground conditions, (such as anomalies) and the properties of soil and rock (such as porosity, saturation, and pore fluid characteristics). The shape of electrodes used in an electrical resistivity survey depends on the purpose of the survey and installation conditions. Most electrodes for field applications are cylindrical for sufficient contact with the ground, while some are conically sharpened at their tips for convenient penetration. Previous study only derived theoretical equations for rod-shaped electrodes with spherical tips. In this study, the theoretical resistance for two cylindrical electrodes with conical tips is derived and verified experimentally. The influence of the penetration depth and tip on the measurement is also discussed.

Keywords: cylindrical electrode; electrical resistance; electrode tip; penetration depth

1. Introduction

The electrical resistivity method has been commonly utilized 1) to evaluate ground properties such as porosity, degree of saturation and pore fluid chemistry, 2) to estimate migration of fluid such as moisture and cement grout and 3) to predict anomalies (Wenner 1912, Tagg 1964, Telford *et al.* 1990, Byun *et al.* 2019, Lee *et al.* 2021, Lei *et al.* 2021, Jo *et al.* 2019, Lee *et al.* 2019, Lee *et al.* 2020). The number of electrodes and arrangement of the potential and current electrodes vary with the purpose of the electrical resistivity survey while the electrode shapes are changed according to measurement conditions. Flat electrodes are specifically utilized in case of paved surface, however, cylindrical electrodes are adopted to obtain sufficient contact area with medium to minimize the grounding resistance in general (Moussa *et al.* 1977, Athanasiou *et al.* 2007, Ruicker *et al.* 2006). The tip of the electrodes are usually sharpened to penetrate conveniently (Cho *et al.* 2004). The theoretical electrical resistance between two cylindrical electrodes was obtained from our previous research (Hong *et al.* 2019). However, the widely utilized sharpened tip is not taken into account for derivation of theoretical resistance between two rod-shaped electrodes. In this study, electrical resistance is theoretically derived for cylindrical electrodes with conical tips to reflect precise test conditions. Experimental tests are conducted to verify the theoretical equation and compare the obtained data with that of cylindrical electrodes with a spherical tip.

---

*Corresponding author, Professor
 E-mail: shchong@scnu.ac.kr
[a]Ph.D.
 E-mail: chhong@kaeri.re.kr
[b]Ph.D.
 E-mail: kjs@kaeri.re.kr

2. Theoretical background

2.1 Electrical resistance from two cylindrical electrodes with spherical tips

The electrical resistance of the two electrodes (R) can be derived from the difference in potential between two oppositely polarized electrodes (V_+: potential of the positively polarized electrode, V_-: potential of the negatively polarized electrode, I: current flow between the two electrodes, Eq. (1)).

$$R = \frac{V_+ - V_-}{I} \tag{1}$$

The potential of an electrode can be obtained from the equipotential surface area $A(x)$ of the electrodes (Eq. (2)).

$$V = \int \frac{\rho I}{A(x)} dx \tag{2}$$

The equipotential surface area is expressed as the shortest distance from the electrode surface to an arbitrary point (x). The equipotential surface area of a single cylindrical electrode with a spherical tip is (Fig. 1)

$$A_s(x) = \underbrace{2\pi(r+x)l}_{\text{cylinder side}} + \underbrace{2\pi(r+x)^2}_{\text{Half sphere}} \tag{3}$$

The electric potentials of two cylindrical electrodes with spherical tips can be derived using the following equation

$$V_1 = -V_2 = \int_0^{L-2r} \frac{\rho I}{A_s(x)} dx = \frac{\rho I}{2\pi l}\left[\ln\left(1+\frac{l}{r}\right) - \ln\left(1+\frac{l}{L-r}\right)\right] \tag{4}$$

V_1 is the potential of the positively charged electrode, V_2 is the potential of the negatively charged electrode, ρ is the electrical resistivity of the target media, I is the electric current flowing between the two electrodes, L is the distance between the two electrodes.

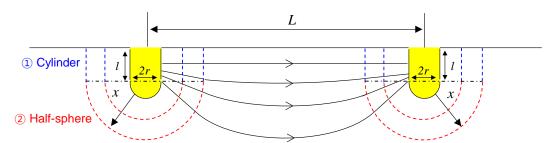The electrical resistance of two rod-shaped electrodes

Fig. 1 Definitions of the terms and shape of equipotential surface between two cylindrical electrodes with spherical tip (Modified from Hong *et al.* 2019)
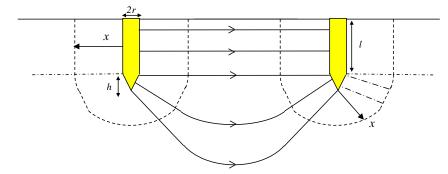

Fig. 2 Definitions of the symbols and equipotential surface shape between two cylindrical electrodes with conical tip

with spherical tips (R_s) is

$$R_s = \frac{V_1 - V_2}{I} = \frac{\rho}{\pi l}\left[\ln\left(1 + \frac{l}{r}\right) - \ln\left(1 + \frac{l}{L-r}\right)\right] \quad (5)$$

where ρ is the electrical resistivity of the medium, l is the penetration depth of the electrodes into the medium, r is the electrode radius, and L is the distance between the two electrodes.

2.2 Electrical resistance from two cylindrical electrodes with conical tips

The equipotential surface area of rod electrodes with conical tip, $A_c(x)$ is composed of cylinder perimeter, part of outer torus, truncated cone, and part of sphere as shown in Fig. 2. The detailed derivation of the equipotential surface area is explained in Appendix A.

$$A_c(x) = 2\pi x^2 + 2\pi(h + r\tan^{-1}(r/h) + l)x + \pi r\left(\sqrt{h^2 + r^2} + 2l\right) \quad (6)$$

The electric potentials obtained from two electrodes with conical tip are evaluated as the following equations.

$$V_3 = -V_4 = \int_0^{L-2r} \frac{\rho I}{A_c(x)}dx = \frac{\rho I}{2\pi(C_2 - C_1)}\left[\ln\frac{C_1}{C_2} - \ln\frac{L-2r+C_1}{L-2r+C_2}\right]$$

$$C_1 = \frac{h + r\tan^{-1}\left(\frac{r}{h}\right) + l - \sqrt{\left(h + r\tan^{-1}\left(\frac{r}{h}\right) + l\right)^2 - 2r\left(\sqrt{h^2 + r^2} + 2l\right)}}{2} \quad (7)$$

$$C_2 = \frac{h + r\tan^{-1}\left(\frac{r}{h}\right) + l + \sqrt{\left(h + r\tan^{-1}\left(\frac{r}{h}\right) + l\right)^2 - 2r\left(\sqrt{h^2 + r^2} + 2l\right)}}{2}$$

where V_3 and V_4 are the potential from positive and negative polarity electrodes, C_1 and C_2 are constants.

Then, the electrical resistance from two cylindrical

electrodes with conical tips is

$$R_c = \frac{\rho}{\pi(C_2 - C_1)}\left[\ln\frac{C_2}{C_1} - \ln\frac{L-2r+C_2}{L-2r+C_1}\right] \quad (8)$$

2.3 Electrical resistance from two conical tip cylindrical electrodes near the non-conductive boundary

Electrical resistance increases near a non-conductive boundary (Park *et al.* 2017). The boundary effect can be explained by using 'method of image' to force potential variation on the boundary zero by placing imaginary electrodes on the opposite side of the boundary as Fig. 3 (Hong *et al.* 2019). The electric potential of cylindrical electrodes with conical tips in an equivalent system is

$$V_5 = \frac{\rho I}{2\pi(C_2 - C_1)}\left[\underbrace{\ln\frac{C_2}{C_1} - \ln\frac{L-2r+C_2}{L-2r+C_1}}_{\text{Effect of two real electrodes}} + \left(\underbrace{\ln\frac{W_1 - L - 2r + C_2}{W_1 - L - 2r + C_1}}_{\text{Effect of M'}}\right) + \left(\underbrace{-\ln\frac{W_1 - 2r + C_2}{W_1 - 2r + C_1}}_{\text{Effect of N'}}\right) + \left(\underbrace{\ln\frac{W_1 + L - 2r + C_2}{W_1 + L - 2r + C_1}}_{\text{Effect of M''}}\right) + \left(\underbrace{-\ln\frac{W_1 - 2r + C_2}{W_1 - 2r + C_1}}_{\text{Effect of N''}}\right)\right] \quad (9)$$

$$V_6 = \frac{\rho I}{2\pi(C_2 - C_1)}\left[\underbrace{-\ln\frac{C_2}{C_1} + \ln\frac{L-2r+C_2}{L-2r+C_1}}_{\text{Effect of two real electrodes}} + \left(\underbrace{-\ln\frac{W_1 - L - 2r + C_2}{W_1 - L - 2r + C_1}}_{\text{Effect of N''}} + \underbrace{\ln\frac{W_1 - 2r + C_2}{W_1 - 2r + C_1}}_{\text{Effect of M''}}\right) + \left(\underbrace{-\ln\frac{W_1 + L - 2r + C_2}{W_1 + L - 2r + C_1}}_{\text{Effect of N'}} + \underbrace{\ln\frac{W_1 - 2r + C_2}{W_1 - 2r + C_1}}_{\text{Effect of M'}}\right)\right] \quad (10)$$
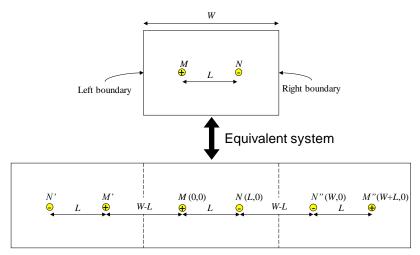
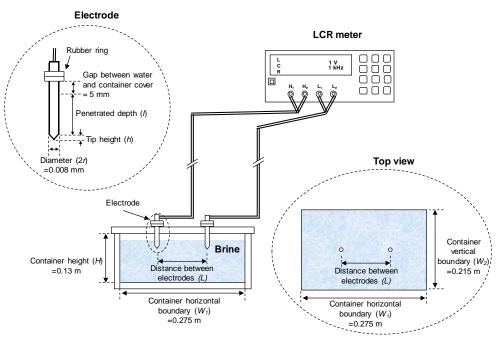Fig. 3 Equivalent system with imaginary electrodes (Hong *et al*. 2019)

Fig. 4 Test setup: measurement equipment, container and electrodes

where W_1 is the width of the container in the moving direction of the electrodes.

The electrical resistance from two cylindrical electrodes with conical tips is

$$R_{c-boundary} = \frac{V_5 - V_6}{I} = \frac{\rho}{\pi(C_2 - C_1)} \left[\underbrace{\ln\frac{C_2}{C_1} - \ln\frac{L-2r+C_2}{L-2r+C_1}}_{\text{Effect of two real electrodes}} + \underbrace{\ln\frac{W-L-2r+C_2}{W-L-2r+C_1} + \ln\frac{W+L-2r+C_2}{W+L-2r+C_1} - 2\ln\frac{W-2r+C_2}{W-2r+C_1}}_{\text{Effect of boundaries}} \right] \quad (11)$$

3. Experimental tests and results

Experimental tests are conducted to verify the derived theoretical equation. Saline water, prepared by adding 0.4 g NaCl (0.001 moles/liter) to distilled water, is employed to constantly maintain electrical resistivity. The electrical resistivity of the saline water, measured using a pH/conductivity meter (Mettler Toledo S213), is 1,454 Ωm. Fig. 4 presents the test setup for the electrical resistance measurement using an LCR meter (Agilent HP 4263 B). The water container (0.275×0.215×0.13 m³) is made of non-conductive acrylic. The cylindrical electrodes are made of stainless steel (SUS303) to avoid corrosion and, rubber rings are used to manage the penetration depth of the electrodes. The electrodes measured 4 mm in radius (r), 50 mm in penetration depth (l), and 4 mm in conical tip height (h). An electric signal of 1 V and 1 kHz is induced to avoid the polarization effect (Glover *et al*. 2002, McCarter *et al*. 2009). The electrical resistance is obtained by changing the depth of penetration (l) and distance between the two rod-shaped electrodes (L). The test cases are listed in Table 1.

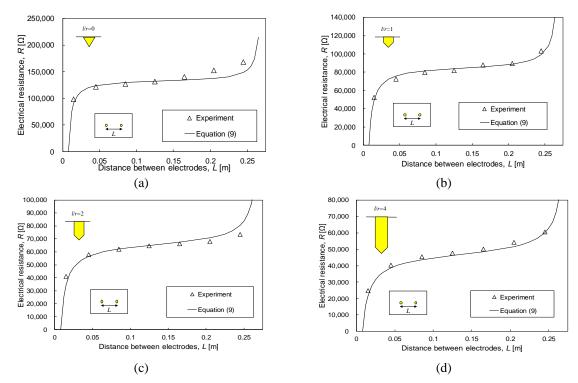The electrical resistance is depicted along the distance

Fig. 5 Electrical resistance of different distance and depth: (a) l/r=0, (b) l/r =1, (c) l/r =2, and (d) l/r =4. Radius (r) and tip height (h) are fixed as 0.004 m. and penetration depth (l) varies from 0 to 0.016 m

Table 1 Experimental test cases

Electrical resistivity, ρ [Ωm]	Penetration depth, l [mm]	Distance between two electrodes, L [m]
1,454	0 4 8 16	0.015 0.045 0.085 0.125 0.165 0.205 0.245

between the two rod-shaped electrodes with conical tips (Fig. 5). Longer distance between two electrodes produces higher electrical resistance in all cases. Particularly, deeply penetrated electrodes offer a lower measured resistance because of their higher contact area. Overall, the distance between the two electrodes, the penetration depth, and the theoretical resistance from Eq. (11) offer a strong expectation of experimental resistance.

4. Discussion

4.1 Electrical resistance between spherical and conical tip electrodes

The electrical resistance between the two rod-shaped electrodes with conical tips is compared to the electrical resistance between the two cylindrical electrodes with spherical tips. It can be assumed that two cylindrical electrodes with conical tips can be treated as cylindrical electrodes with spherical tips at certain depths. To compare the two theoretical equations in the parametrical, we
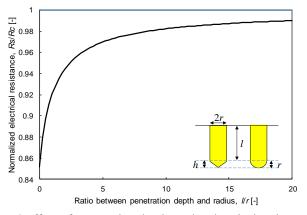

Fig. 6 Effect of penetration depth on the electrical resistance of spherical and conical tip cylindrical electrodes. Distacne between two electrodes is fixed as 0.085 m

assumed that two pairs of cylindrical electrodes, one with a conical tip (h=4 mm) and the other with a spherical tip (r=4 mm) are separated by a distance of 0.085 m (Fig. 6). The electrical resistances of the two pairs of electrodes are normalized and plotted as the ratio between the penetration depth and radius of the electrodes. When only tips were penetrated (l/r=0), the electrical resistance of the conical tip electrodes and spherical tip electrodes differed by approximately 15%. As the electrodes penetrate more, the normalized electrical resistance tends to become unity. If we allow a 2% difference (R_s/R_c > 0.98), we can treat the cylindrical electrodes with conical tips as electrodes with spherical tips when l/r is greater than 9.

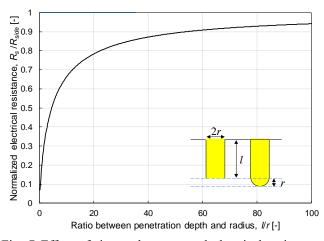### 4.2 Effect of tip on electrical resistance measurement

Fig. 7 Effect of tip on the measured electrical resistance. Distacne between two electrodes is fixed as 0.085 m

The current flow between two cylindrical electrodes can be treated as 2-dimensional when the penetration of the electrodes is sufficiently deep (Jaschinsky *et al*. 2008). The influence of the tip on the electrical resistance is analyzed by comparing the theoretical resistances between two pairs of cylindrical electrodes with and without a tip. We can simply calculate the equipotential surface area without the tip as $\pi(r+x)l$ and the electric potential of the cylindrical electrodes without the tip are as follows

$$V_7 = -V_8 = \int_0^{L-2r} \frac{\rho I}{2\pi(r+x)l} dx = \frac{\rho I}{2\pi l} \ln\left(\frac{L-r}{r}\right) \qquad (12)$$

where V_7 and V_8 are the potentials from the positively and negatively charged electrodes, respectively.

The electrical resistance between two rod-shaped electrodes without tip (R_{side}) is

$$R_{side} = \frac{\rho}{\pi l} \ln\left(\frac{L-r}{r}\right) \qquad (13)$$

Note that cylindrical electrodes with conical tips can be treated as spherical tips when l/r exceeds 9 within a 2% error. Cylindrical electrodes with spherical tips can be a representative tip shape. The normalized electrical resistance (R_s/R_{side}) is

$$\frac{R_s}{R_{side}} = \frac{\frac{\rho}{\pi l}\left[\ln\left(1+\frac{l}{r}\right)-\ln\left(1+\frac{l}{L-r}\right)\right]}{\frac{\rho}{\pi l}\ln\left(\frac{L-r}{r}\right)} = \frac{\ln\left(\frac{(l+r)(L-r)}{r(L-r+l)}\right)}{\ln\left(\frac{L-r}{r}\right)} \qquad (14)$$

It is clear that when l approaches infinity, R_s becomes R_{side}. It is assumed that the electrode radius and arrangement are identical to those in the previous section, and only the penetration depth is varied in the parametric study (Fig. 7). When l/r is 10, representing the cylindrical electrodes with spherical and conical tips as identical, the electrical resistance between the cylindrical electrodes with spherical tips and without a tip shows a significant gap of approximately 0.35 (35% error). Even at a very deep penetration depth (l/r=100), the electrical resistance between the two cylindrical electrodes with spherical tips and without a tip still had a difference of more than 5%. This implies that even though cylindrical electrodes with conical tips can be treated as cylindrical electrodes with spherical tips, the tip should be considered to evaluate the

theoretical equation of the cylindrical electrodes in deeply penetrated conditions. Note that similar trend is observed with conical tip because higher l/r deletes the tip shape effect.

5. Conclusions

The theoretical electrical resistance between two cylindrical electrodes with conical tip is derived. Experimental tests are conducted to verify the theoretical equations. Our findings can be summarized as follows.
• The theoretical electrical resistance between two cylindrically shaped electrodes with conical tip is represented with the radius (r), penetration depth (l) and tip height (h) of the electrodes and the distance between two electrodes (L). Higher electrical resistance is produced with longer distance between two electrodes, smaller electrode radius and tip height, and shallower penetration depth.
• The theoretical electrical resistance between two cylindrical electrodes with conical tip and spherical tip is compared in various penetration depths. The cylindrical electrodes with conical tips can be treated as the cylindrical electrodes with spherical tip within 2% error which provides a simpler theoretical form of the electrical resistance when the ratio between the penetration depth and radius is greater than 9.
• Previous studies neglect the tip in calculation of theoretical electrical resistance, however, the tip affect more than 30% of the theoretical electrical resistance when l/r=9. Even in the deeply penetrated conditions (l/r=100), the tip affects the resultant electrical resistance by more than 5%. Therefore, the tip should be carefully considered when evaluating the theoretical electrical resistance between two cylindrical electrodes.
• In laboratory tests for electrical resistivity measurement, calibration tests are required to obtain shape factor (i.e., calibration factor) for the conversion of measured electrical resistance into electrical resistivity (Oh *et al*. 2015, Choo *et al*. 2016). The theoretical formulation under the same experimental condition (electrode geometry and container size) can replace the cumbersome calibration procedures if the electrical resistance can be analytically obtained (Hong *et al*. 2019, Hong *et al*. 2020)

References

Athanasiou, E.N., Tsourlos, P.I., Vargemezis, G.N., Papazachos, C.B. and Tsokas, G.N. (2007), "Non-destructive DC resistivity

surveying using flat-base electrodes", *Near Surf. Geophys.*, **5**, 273-282. https://doi.org/10.3997/1873-0604.2007008.

Byun, Y.K., Hong, W.T. and Yoon, H.K. (2019), "Characterization of cementation factor of unconsolidated granular materials through time domain reflectometry with variable saturated conditions", *Mater.*, **12**, 1340. https://doi.org/10.3390/ma12081340.

Cho, G.C., Lee, J.S. and Santamarina, J.C. (2004) "Spatial variability in soils: high resolution assessment with electrical needle probe", *J. Geotech. Geoenvir.*, **130**, 843-850. https://doi.org/10.1061/(ASCE)1090-0241(2004)130:8(843).

Choo, H., Song, J., Lee, W. and Lee, C. (2016), "Impact of pore water conductivity and porosity on the electrical conductivity of kaolinite", *Acta Geotech.*, **11**, 1419-1429. https://doi.org/10.1007/s11440-016-0490-4.

Glover, P.W.J., Hole, M.J. and Pous, J. (2000), "A modified Archie's law for two conducting phases", *Earth Planet. Sci. Let.*, **180**, 369-383. https://doi.org/10.1016/S0012-821X(00)00168-0.

Hong, C.H., Chong, S.H. and Cho, G.C. (2019), "Theoretical study on geometries of electrodes in laboratory electrical resistivity measurement", *Appl. Sci.*, **9**, 4167. https://doi.org/10.3390/app9194167.

Hong, C.H., Chong, S.H. and Cho, G.C. (2020), "Electrical resistivity measurement with spherical-tipped cylindrical electrode embedded on two layers", *Mater.*, **13**, 2144. https://dx.doi.org/10.3390/ma13092144,

Jaschinsky, P., Wensorra, J., Lepsa, M.I., Mysliveček, J. and Voigtländer, B. (2008) "Nanoscale charge transport measurements using a double-tip scanning tunneling microscope". *J. Appl. Phys.*, **104**, 094307. https://doi.org/10.1063/1.3006891,

Jo, S.A., Kim, K.Y. and Ryu, H.H. (2019), "A new geophysical exploration method based on electrical resistivity to detect underground utility lines and geological anomalies: Theory and field demonstrations", *Geomech. Eng.*, **18**(5), 527-534. https://doi.org/10.12989/gae.2019.18.5.527.

Lee, H.B., Oh, T.M. and Lee, J.W. (2021), "Evaluation of grout penetration in single rock fracture using electrical resistivity", *Geomech. Eng.*, **24**(1), 1-14. https://doi.org/10.12989/gae.2021.24.1.001.

Lee, K.H., Park, J.H., Park, J., Lee, I.M. and Lee, S.W. (2019), "Electrical resistivity tomography survey for prediction of anomaly in mechanized tunneling", *Geomech. Eng.*, **19**(1), 93-104. https://doi.org/10.12989/gae.2019.19.1.093.

Lee, K.H., Park, J.H., Park, J., Lee, I.M. and Lee, S.W. (2019), "Experimental verification for prediction method of anomaly ahead of tunnel face by using electrical resistivity tomography", *Geomech. Eng.*, **20**(6), 475-484. https://doi.org/10.12989/gae.2020.20.6.475.

Lei, J., Chen, W., Li, F., Yu, H., Ma, Y. and Tian, Y. (2021), "Investigation on moisture migration of unsaturated clay using cross-borehole electrical resistivity tomography technique", *Geomech. Eng.*, **25**(4), 295-302. https://doi.org/10.12989/gae.2021.25.4.295.

McCarter, W. J., Starrs, G., Kandasami, S., Jones, R. and Chrisp, T. (2009), "Electrode configurations for resistivity measurements on concrete", *ACI Mat. J.*, **106**, 258-264. https://doi.org/10.14359/56550.

Moussa, A.H., Dolphin, L.T. and Mokhtar, G. (1977), "Applications of modern sensing techniques to Egyptology", Report of the 1977 Field Experiments by a Joint Team, SRI International, Menlo Park, California.

Oh, T.M., Cho, G.C., Son, T.A., Ryu, H.H. and Lee, C. (2015), "Experimental approach to evaluate weathering condition of granite using electrical resistivity", *Geomech. Eng.*, **8**(5), 675-685. https:// doi.org/10.12989/gae.2015.8.5.675.

Park, J., Lee, K.H., Seo, H., Ryu, J. and Lee, I.M. (2017), "Role of

induced electrical polarization to identify soft ground/fractured rock conditions", *J. Appl. Geophys.*, **137**, 63-72. https://doi.org/10.1016/j.jappgeo.2016.12.017.

Rücker, C., Günther, T. and Spitzer, K. (2006), "Three-dimensional modelling and inversion of dc resistivity data incorporating topography-I. Modelling", *Geophys. J. Int.*, **166**, 495-505. https://doi.org/10.1111/j.1365-246X.2006.03010.x.

Tagg, G.F. (1964), *Earth Resistances*, Pitman Pub., Corp., New York.

Telford, W.M., Geldart, L.P. and Sheriff, R.E. (1990), *Applied Geophysics*, 2nd Edition, Cambridge University Press, Cambridge.

Wenner, F. (1912), "The four-terminal conductor and the Thomson bridge", *J. Washington Acad. Sci.*, **2**(3), 63-65.

IC

Appendix A. Derivation of the equipotential surface area of cylindrical electrodes with conical tips

The equipotential surface area is represented in terms of the distance from the electrode surface (x). Because the equipotential surface area of the conical tip electrode is composed of a cylinder, part of the outer torus, a truncated cone, and part of the half-sphere, the surface area is calculated by summing, as follows

$$
\begin{aligned}
A_c(x) =\ & \underbrace{2\pi x + r(l)}_{1.\ \text{Cylinder}} + \underbrace{\pi^2 rx + 2\pi x^2\left(\tan^{-1}\frac{r}{h}\right)}_{2.\ \text{Part of outer torus}} = \theta,\ \pi-2\theta \\
& + \underbrace{\pi\left(r + x\ \frac{h}{\sqrt{h^2 + r^2}} = \cos\theta + x\ \frac{h}{\sqrt{h^2 + r^2}}\right)\sqrt{h^2 + r^2}}_{3.\ \text{Truncated cone}} \\
& + \underbrace{2\tan^{-1}\frac{r}{h}\ x^2}_{4.\ \text{part of sphere}} \\
=\ & 2\pi x^2 + 2\pi\left(h + r\tan^{-1}\frac{r}{h}\right) + l(x + \pi r)\left(\frac{h}{\sqrt{h^2 + r^2}} + 2l\right)
\end{aligned}
\tag{A1}
$$

The equipotential surface area of the partial outer torus affected the cone height and radius. The lateral area of the truncated cone can be calculated using the slant height ($\sqrt{h^2 + r^2}$), the sum of the base radius ($r + x\cos\theta$), and the top radius ($x\cos\theta$). The partial sphere's equipotential area is $\pi-2\theta$ multiplied by the surface area of the half sphere ($2\pi x^2$).
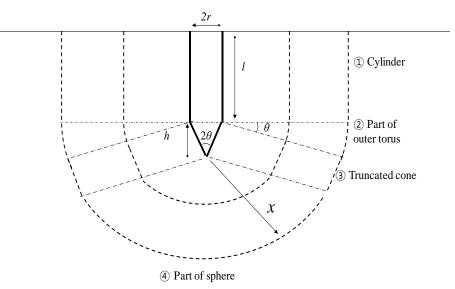

④ Part of sphere

Fig. A1 Symbols of the cylindrical electrodes with conical tip